

Search for Heavy Neutral Leptons with IceCube DeepCore

Dissertation
zur Erlangung des akademischen Grades
doctor rerum naturalium
(Dr. rer. nat.)

im Fach: Physik
Spezialisierung: Experimentalphysik

eingereicht an der
Mathematisch-Naturwissenschaftlichen Fakultät
der Humboldt-Universität zu Berlin

von
Leander Fischer M. Sc.
geboren am 24. Oktober 1992
in Heidelberg

Präsidentin der Humboldt-Universität zu Berlin
Prof. Dr. Julia von Blumenthal

Dekanin der Mathematisch-Naturwissenschaftlichen Fakultät
Prof. Dr. Caren Tischendorf

Copyright Notice

This book is released into the public domain using the CC-BY-4.0 code.

To view a copy of the CC-BY-4.0 code, visit:

<https://creativecommons.org/licenses/by/4.0/>

Colophon

This document was typeset with the help of KOMA-Script and L^AT_EX using the open-source kaobook template class.

The source code of this thesis is available at:

https://github.com/LeanderFischer/phd_thesis

Zusammenfassung

Zusammenfassung ...

Abstract

Abstract ...

Todo list

| | |
|---|----|
| (Re-)write SM neutrino chapter for PhD thesis (just copy paste from M.Sc.) | 1 |
| Plot is missing + for W and 0 for Z boson | 2 |
| SB: It seems that you have some double counting of information here . I suggest to move some of the information in this "intro" paragraph to the appropriate subsections | 2 |
| Explain momenta and momentum transfer (p,q) in these figures. | 4 |
| SB: Somehow all of this needs to come much sooner in the thesis. Oscillations are the way that you get your nutau flux, so they should be explained, but it should not exceed nor proceed the HNL theory and pheno discussion | 4 |
| Re-write/re-formulate this section (copied from HNL technote). | 4 |
| Produce similar styled plot for these limits | 4 |
| This section really needs to be re-written to motivate the search for HNLs from a more generic point of view (e.g. to explain neutrino masses) | 4 |
| This section definitely needs to be elaborated in a little more detail | 5 |
| Not adding information about the case where the neutrinos have Dirac or pseudo-Dirac masses | 5 |
| (Re-)write BSM chapter for PhD thesis (just copy paste from M.Sc.) | 8 |
| SB: You could say why with an extra half-sentence. | 8 |
| SB: I don't think this is true - the normalization is known to 5% if you trust Anatoli/Juan Pablo. Please have a look at more recent publications on this topic. | 9 |
| SB: formatting/margins also I don't think you defined rho1,2 | 9 |
| Make my own DC string positions/distances plot version. | 12 |
| Re-make plot with all energies (cascades and total, both sets (they are the same)) | 13 |
| Re-make plot with all decay lengths (both sets) | 13 |
| Re-make plot with 3 target masses and better labels | 16 |
| Add comparisons of SM cross-sections between NuXSSplMkr and genie? | 17 |
| add varied total cross-section for a few background HNL events (for QE/RES variations?!?) | 17 |
| Calculate max BRs | 17 |
| where is PISA introduced? is there a reference? | 19 |
| add table with number of gen level files? mention the event number is smaller because of kinematic condition? | 20 |
| add information about the matter profile used | 23 |
| add information about the oscillation probability calculation and the software used for it | 23 |
| get correct final level rates from my pipeline(s) | 23 |
| add rate and Poisson error for HNL samples | 23 |
| maybe just pick one mixing? | 23 |
| add 3D expectation and/or S/sqrt(B) plots | 24 |

| | |
|--|----|
| Do I want/need to include the description of the KDE muon estimation? | 24 |
| Add table with all systematic uncertainties used in this analysis (in the analysis chapter). | 24 |
| add final level effects of varying the axial mass parameters (or example of one) | 24 |
| add final level effects of varying the DIS parameter (or example of one) | 24 |
| Do I want additional plots for this (fit diff, LLH distr, minim. stats, param. fits)? | 25 |
| Add bin-wise TS distribution? Add 3D TS maps? | 25 |

Contents

| | |
|---|------------|
| Abstract | iii |
| Contents | vii |
| 1 Standard Model Neutrinos and Beyond | 1 |
| 1.1 Standard Model Particles | 1 |
| 1.1.1 Electroweak Symmetry Breaking | 1 |
| 1.1.2 Fermion Masses | 1 |
| 1.1.3 See-Saw Mechanisms | 1 |
| 1.1.4 Radiative Neutrino Masses | 1 |
| 1.2 Neutrino Properties | 1 |
| 1.2.1 Quantum Numbers | 1 |
| 1.2.2 Mass | 1 |
| 1.2.3 Active Neutrino Flavors | 1 |
| 1.3 Neutrino Interactions | 1 |
| 1.3.1 Weak Interactions after Symmetry-Breaking | 1 |
| 1.3.2 Neutrino-Lepton Scattering | 2 |
| 1.3.3 Neutrino Interactions with Nuclei | 2 |
| 1.4 Heavy Neutral Leptons | 4 |
| 1.4.1 Motivation for Heavy Sterile Neutrinos | 4 |
| 1.4.2 Extending the Standard Model | 5 |
| 1.4.3 Production and Decay in IceCube DeepCore | 7 |
| 1.4.4 Existing Constraints on Mixing | 7 |
| 1.5 Neutrino Oscillations | 8 |
| 1.5.1 Vacuum Oscillations | 8 |
| 1.5.2 Oscillations in Matter | 8 |
| 1.5.3 Atmospheric Neutrino Oscillations | 8 |
| 1.6 Open Questions in Neutrino Particle Physics | 10 |
| 2 Heavy Neutral Lepton Signal Simulation | 11 |
| 2.1 Model Independent Simulation | 11 |
| 2.1.1 Generator Functions | 11 |
| 2.1.2 Simplistic Sets | 12 |
| 2.1.3 Realistic Set | 13 |
| 2.2 Model Dependent Simulation | 15 |
| 2.2.1 Custom LeptonInjector | 15 |
| 2.2.2 Sampling Distributions | 18 |
| 2.2.3 Weighting Scheme | 19 |
| 2.2.4 Generation Level Distributions | 20 |
| 3 Detecting Low Energetic Double Cascades | 21 |
| 3.1 Reconstruction | 21 |
| 3.1.1 Table-Based Minimum Likelihood Algorithms | 21 |
| 3.1.2 Double Cascade Hypothesis | 21 |
| 3.1.3 Modification to Low Energy Events | 21 |
| 3.2 Cross Checks | 21 |
| 3.2.1 Simplistic Sets | 21 |
| 3.3 Performance | 22 |
| 3.3.1 Energy/Decay Length Resolution | 22 |
| 3.3.2 Double Cascade Classification | 22 |

| | | |
|----------|--|-----------|
| 4 | Search for an Excess of Heavy Neutral Lepton Events | 23 |
| 4.1 | Final Level Sample | 23 |
| 4.1.1 | Expected Rates/Events | 23 |
| 4.1.2 | Analysis Binning | 24 |
| 4.2 | Statistical Analysis | 24 |
| 4.2.1 | Test Statistic | 24 |
| 4.2.2 | Systematic Uncertainties | 24 |
| 4.3 | Analysis Checks | 25 |
| 4.3.1 | Minimization Robustness | 25 |
| 4.3.2 | Ensemble Tests | 25 |
| 4.4 | Results | 26 |
| 4.4.1 | Best Fit Parameters | 26 |
| 4.4.2 | Upper Limits | 26 |
| 4.4.3 | Post-Fit Data/MC Agreement | 26 |
| 4.4.4 | Likelihood Coverage | 26 |
| | Bibliography | 27 |

List of Figures

| | | |
|-----|--|----|
| 1.1 | Feynman diagrams of neutrino weak interactions, taken from [4] | 2 |
| 1.2 | Total inclusive neutrino-nucleon cross-sections, taken from [5]. | 3 |
| 1.3 | Neutrino-nucleon deep inelastic scattering, taken from [4] | 4 |
| 1.4 | Current $ U_{\tau 4}^2 $ limits from NOMAD [7], ArgoNeut [8], CHARM [9, 10], and DELPHI [11]. | 5 |
| 1.5 | Production of a sterile neutrino in the up-scattering of a tau neutrino. | 6 |
| 1.6 | Sterile neutrino decay through neutral current (left) and charged current (right). With the current limits on $ U_{e4} ^2$ and $ U_{\mu 4} ^2$ being orders of magnitude stronger than that on $ U_{\tau 4} ^2$ [Atre:2009rg], the decay modes with an electron, an electron neutrino, a muon or a muon neutrino in the final state are not considered. | 6 |
| 1.7 | Branching ratios, decay widths, and proper lifetime of the HNL within the mass range considered, calculated based on the results from [14]. Given the existing constraints on $ U_{e4} ^2$ and $ U_{\mu 4} ^2$, we consider that the corresponding decay modes are negligible. | 7 |
| 1.8 | Decay widths of the HNL within the mass range considered, calculated based on the results from [14]. Given the existing constraints on $ U_{e4} ^2$ and $ U_{\mu 4} ^2$, we consider that the corresponding decay modes are negligible. | 7 |
| 1.9 | Atmospheric neutrino fluxes, taken from [15] | 8 |
| 2.1 | DeepCore string spacing | 12 |
| 2.2 | Simplified model independent simulation generation level distributions | 13 |
| 2.3 | Realistic model independent simulation generation level distributions | 14 |
| 2.4 | HNL branching ratios | 15 |
| 2.5 | Custom HNL total cross-sections for the four target masses compared to the total ($\nu_\tau/\bar{\nu}_\tau$ NC) cross-section used for SM neutrino simulation production with GENIE. | 16 |
| 2.6 | Model dependent simulation generation level distributions | 20 |
| 4.1 | Asimov inject/recover test (0.6 GeV) | 26 |
| 4.2 | Pseudo-data trials TS distribution (0.6 GeV) | 26 |

List of Tables

| | | |
|-----|--|----|
| 2.1 | Simplified model independent simulation sampling distributions | 13 |
| 2.2 | Realistic model independent simulation sampling distributions | 14 |
| 2.3 | HNL mass dependent decay channels | 17 |
| 2.4 | Model dependent simulation sampling distributions | 19 |
| 4.1 | Final level event/rate expectation | 23 |
| 4.2 | Analysis binning | 24 |
| 4.3 | Staged minimization settings | 25 |

Standard Model Neutrinos and Beyond

1

This chapter introduces the basic properties of neutrinos, their place in the Standard Model of particle physics (SM) and their peculiarities following the description of [1].

(Re-)write SM neutrino chapter for PhD thesis (last copy)
11 Standard Model Particles
12 Neutrino Properties . . . 1

13 Neutrino Interactions 1
[1]: Thomson (2013), *Modern particle physics*
14 Heavy Neutral Leptons . . . 4

1.5 Neutrino Oscillations . . . 8

1.6 Open Questions in Neutrino Particle Physics . . . 10

1.1 Standard Model Particles

1.1.1 Electroweak Symmetry Breaking

1.1.2 Fermion Masses

Charged - Leptons and Quarks

Uncharged - Neutrinos

Dirac

Majorana

1.1.3 See-Saw Mechanisms

1.1.4 Radiative Neutrino Masses

1.2 Neutrino Properties

1.2.1 Quantum Numbers

1.2.2 Mass

1.2.3 Active Neutrino Flavors

1.3 Neutrino Interactions

1.3.1 Weak Interactions after Symmetry-Breaking

The neutrino is an elementary particle in the SM [1]. It belongs to the class of leptons, which itself is a subclass of elementary fermions (spin $\frac{1}{2}$ particles). The fermions - six quarks and six leptons - form the matter content of the universe. Quarks take part in all three interaction types (forces) of the SM: strong, weak, and electromagnetic (EM) [2]. The charged leptons - electron, muon, and tau - are subject to the weak and the EM interaction. Neutrinos carry neither electric charge nor color charge and therefore only take part in weak interactions. There are three

[1]: Thomson (2013), *Modern particle physics*

[2]: Glashow (1961), "Partial-symmetries of weak interactions"

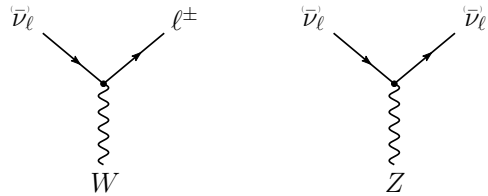


Figure 1.1: Feynman diagrams of charged-current (left) and neutral-current (right) neutrino weak interactions. Taken from [4].

[3]: Tanabashi et al. (2018), "Review of Particle Physics"

Plot is missing + for W and 0 for Z boson.

[1]: Thomson (2013), *Modern particle physics*

distinct neutrino flavors - electron neutrinos, muon neutrinos and tau neutrinos (ν_e , ν_μ , and ν_τ) [3] - each corresponding to their charged lepton counterparts.

In the SM, weak interactions are mediated by the three massive bosons W^+ , W^- , and Z^0 [1]. The large boson masses ($m_W \sim 80$ GeV, $m_Z \sim 90$ GeV) result in a short range of the force of about 10×10^{-18} m. Weak interactions carried by W^\pm bosons are called charged-current (CC) interactions, because charge is transferred between the interacting particles. In CC interactions, a neutrino is converted into its corresponding charged lepton or vice versa. Neutral current (NC) interactions are those mediated by Z^0 bosons. Here no charge is transferred. The Feynman diagrams for CC and NC interactions are shown in Figure 1.1.

Although neutrinos are massless in the SM, we know today that they do have a small mass. The observed phenomenon of neutrino oscillations (see Section Section 1.5) is based on the fact that there is a mass difference between the three neutrino mass eigenstates. From neutrino oscillation measurements the absolute mass scale cannot be determined, since they only depend on the mass differences, but there are upper limits on the sum of all neutrino masses from cosmological observations. These upper limits are typically between 0.3 and 1.3 eV [3].

[3]: Tanabashi et al. (2018), "Review of Particle Physics"

1.3.2 Neutrino-Lepton Scattering

Particle-Antiparticle Scattering

1.3.3 Neutrino Interactions with Nuclei

To describe the neutrino detection principle of IceCube explained in Chapter ?? we need to understand the weak interaction processes that occur at the energies relevant for this work 10 GeV-100 GeV. The cross-sections are dominated by the following neutrino-nucleon interactions: quasi-elastic scattering (QE), resonant scattering (RES), and deep inelastic scattering (DIS). The relative importance of the different processes depends on energy as can be seen in Figure 1.2.

At energies below 5 GeV, QE and RES occur and the neutrinos interact with approximately point-like protons and neutrons. The cross-sections of these processes are not linear in energy and the transition region to higher energies is poorly understood. At higher energies, the interactions are dominated solely by DIS which has a linear dependence on energy above ~ 20 GeV. For a given neutrino energy, it is possible to predict the cross-section in this region. Here neutrinos interact with a single quark, breaking apart the nucleus and producing a shower of relativistic secondary particles. Neutrino DIS is the primary detection channel of

SB: It seems that you have some double counting of information here . I suggest to move some of the information in this "intro" paragraph to the appropriate subsections

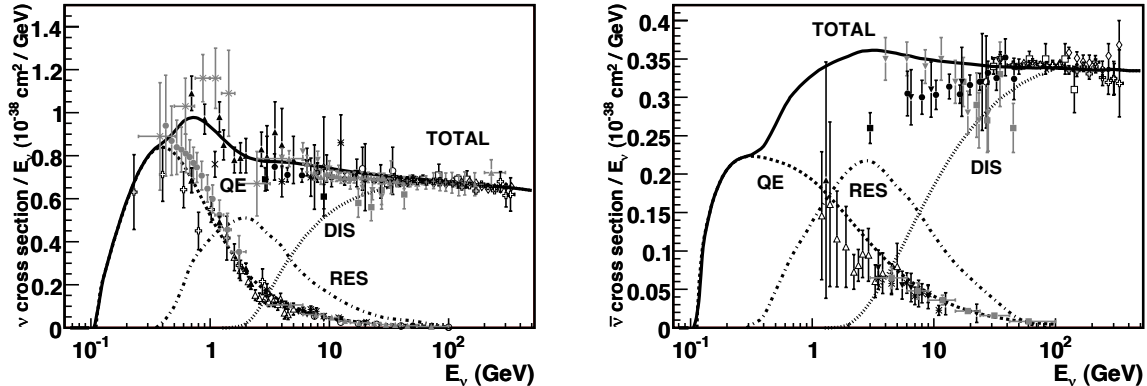


Figure 1.2: Total neutrino(left) and antineutrino(right) per nucleon cross-section divided by neutrino energy plotted against energy. The three main scattering processes quasi-elastic scattering (QE), resonant scattering (RES), and deep-inelastic scattering (DIS) are depicted. Taken from [5].

IceCube. From Figure 1.2 it can be seen that the interaction cross-sections are very small of the order of 10^{-38} cm^2 . Because of the small interaction cross-section, very large volume detectors are required to capture a sufficiently large sample of neutrinos to use for precision studies of their properties. For example, the interaction length of a neutrino with $E_\nu = 10 \text{ GeV}$ is of $\mathcal{O}(10^{10} \text{ km})$.

Charged-current Quasi-elastic Scattering

Quasi-elastic scattering (QE) with nucleons is the main process below 1 GeV. Protons are converted to neutrons in antineutrino interactions and vice-versa for neutrino interactions. Additionally, a charged lepton corresponding to the neutrino/antineutrino flavor is produced.

Resonant Scattering

Resonant scattering (RES) describes the process of a neutrino scattering off a nucleon producing an excited state of the nucleon in addition to a charged lepton. RES is the leading process at $1.5 \times 10^{-5} \text{ GeV}$ for neutrinos and $1.5 \times 10^{-8} \text{ GeV}$ for antineutrinos.

Deep Inelastic Scattering

Deep inelastic scattering (DIS) occurs if a neutrino carries sufficient energy to resolve the underlying structure of the nucleon and interacts with one of the composing quarks. DIS is the dominant process above 10 GeV. The nucleon breaks up and a lepton accompanied by a set of hadronic final states is produced. Whether the lepton is the charged lepton corresponding to the interacting neutrino type, or the neutrino itself depends on the type of DIS interaction. DIS happens via CC as in

$$\begin{aligned} \nu_l + N &\rightarrow l^- + X, \\ \bar{\nu}_l + N &\rightarrow l^+ + X, \end{aligned} \tag{1.1}$$

or NC interactions as

$$\nu_l + N \rightarrow \nu_l + X. \tag{1.2}$$

Here, X stands for any set of final state hadrons and N for the nucleon. The Feynman diagrams for the processes in Equation 1.1 and Equation 1.2 are shown in Figure 1.3.

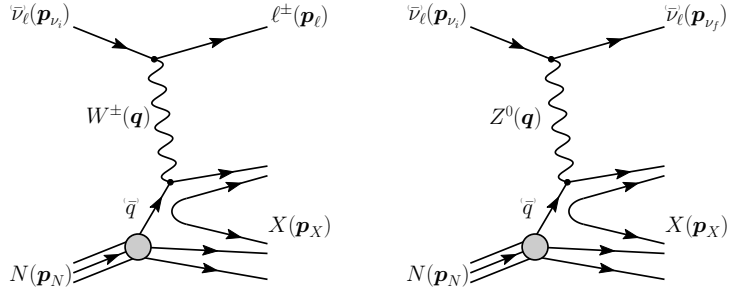


Figure 1.3: Feynman diagrams for deep inelastic scattering of a neutrino with a nucleon via charged-current (left) and neutral current (right) interactions. Taken from [4].

Explain momenta and momentum transfer (p, q) in these figures.

SB: Somehow all of this needs to come much sooner in the thesis. Oscillations are the way that you get your nutau flux, so they should be explained, but it should not exceed nor proceed the HNL theory and pheno discussion

Re-write/re-formulate this section (copied from HNL technote).

[6]: Yanagida (1980), "Horizontal Symmetry and Masses of Neutrinos"

Produce similar styled plot for these limits

[12]: Coloma et al. (2017), "Double-Cascade Events from New Physics in Icecube"

[12]: Coloma et al. (2017), "Double-Cascade Events from New Physics in Icecube"

[13]: Coloma (2019), "Icecube/DeepCore tests for novel explanations of the MiniBooNE anomaly"

This section really needs to be re-written to motivate the search for HNLs from a more generic point of view (e.g. to explain neutrino masses)

1.4 Heavy Neutral Leptons

1.4.1 Motivation for Heavy Sterile Neutrinos

Extensions to the Standard Model (SM) that add *Heavy Neutral Leptons* (HNLs) provide a good explanation for the origin of neutrino masses through different seesaw mechanisms [6]. While the mixing with $\nu_{e/\mu}$ is strongly constrained ($|U_{\alpha 4}^2| \lesssim 10^{-5} - 10^{-8}$, $\alpha = e, \mu$), the mixing with ν_τ is much harder to probe due to the difficulty of producing and detecting ν_τ . Figure 1.4 shows the current limits on the τ -sterile mixing space for HNL masses between 0.1 GeV-10 GeV. As was first pointed out in [12], the atmospheric neutrino flux observed in IceCube offers a way to constrain the neutrino-HNL mixing parameters. By using the large fraction of atmospheric ν_μ events that oscillate into ν_τ before they reach the detector, the less constrained τ -sterile mixing space can be explored. In this document, we present the methodology and strategy of a search for HNLs with IceCube DeepCore. These additional *right-handed* (RH) neutrinos can be included in the Standard Model (SM) by extending the PMNS matrix to at least a 3x4 matrix as

$$\begin{pmatrix} \nu_e \\ \nu_\mu \\ \nu_\tau \end{pmatrix} = \begin{pmatrix} U_{e1} & U_{e2} & U_{e3} & U_{e4} \\ U_{\mu 1} & U_{\mu 2} & U_{\mu 3} & U_{\mu 4} \\ U_{\tau 1} & U_{\tau 2} & U_{\tau 3} & U_{\tau 4} \end{pmatrix} \begin{pmatrix} \nu_1 \\ \nu_2 \\ \nu_3 \\ \nu_4 \end{pmatrix}, \quad (1.3)$$

where the components with index 4 define the mixing between the flavor states and the fourth sterile mass state, respectively. Note here that this is not a theoretically fully consistent picture, but rather the phenomenologically minimal model to be tested by this analysis. This can hopefully be put into the larger context of several fully consistent models, later. Due to the singlet nature of the RH neutrinos, they only interact weakly, inheriting these interactions from their *left-handed* (LH) neutrino counterparts via mixing. This mixing of the HNLs with the electron, muon, and tau neutrinos can be probed and constrained as a function of the HNL mass by searching for their production and decay. In [12, 13] this search is mainly motivated through two experimental arguments. Secondly, IceCube is ideally placed to explore the yet unconstrained

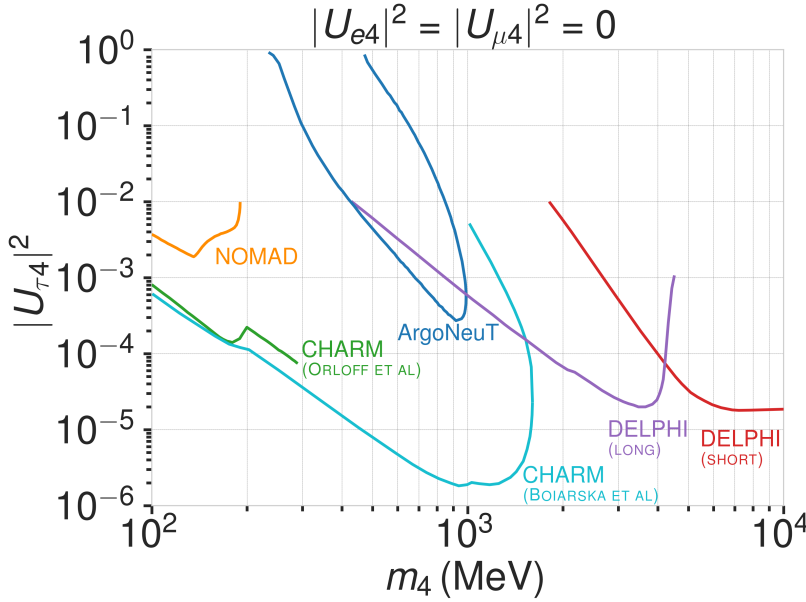


Figure 1.4: Current $|U_{\tau 4}^2|$ limits from NOMAD [7], ArgoNeut [8], CHARM [9, 10], and DELPHI [11].

$|U_{\tau 4}|^2 - m_4$ phase-space that is not easily accessible by accelerator-based experiments.

1.4.2 Extending the Standard Model

In order to probe the τ -sterile mixing parameter, it is required to look at interactions involving τ neutrinos. However, most neutrinos produced in cosmic ray interactions with the atmosphere are ν_e or ν_μ . Therefore, we need these neutrinos to oscillate to the τ flavor before reaching the detector. For this to happen at the considered energies a traveled distance of the order of the earth diameter is necessary. This is why our signal is mostly up-going and passing through the whole earth.

To explain the signature we can observe in IceCube we first have to revisit the weak interactions that the HNL inherits from its LH counterpart through mixing. We will be following the derivation in [14]. Extending the SM by n additional RH neutrinos, ν_i ($i = 3 + n$), leads to the mass Lagrangian

$$\mathcal{L}_\nu^{\text{mass}} \supset - \sum_{\alpha=e,\mu,\tau} \sum_{i=4}^{3+n} Y_{\nu,\alpha i} \bar{L}_{L,\alpha} \tilde{\phi} \nu_i - \frac{1}{2} \sum_{i=4}^{3+n} M_i \bar{\nu}_i \nu_i^c + \text{h.c.}, \quad (1.4)$$

in a basis where the Majorana mass terms are diagonal. $Y_{\nu,\alpha i}$ are the Yukawa couplings to the lepton doublets and M the Majorana masses for the heavy singlets. $L_{L,\alpha}$ stands for the SM LH lepton doublet of flavor α while ϕ is the Higgs field, and $\tilde{\phi} = i\sigma_2\phi^*$ and $\nu_i^c \equiv C\bar{\nu}_i^t$, with $C = i\gamma_0\gamma_2$ in the Weyl representation. The full neutrino mass matrix with the Higgs vacuum expectation value $v/\sqrt{2}$ reads

$$\mathcal{M} = \begin{pmatrix} 0_{3 \times 3} & Y_\nu v / \sqrt{2} \\ Y_\nu^t v / \sqrt{2} & M \end{pmatrix}, \quad (1.5)$$

and can be diagonalized by a $(3 + n) \times (3 + n)$ full unitary rotation U , that itself leads to neutrino masses upon diagonalization, additionally

This section definitely needs to be elaborated in a little more detail

[14]: Coloma et al. (2021), “GeV-scale neutrinos: interactions with mesons and DUNE sensitivity”

Not adding information about the case where the neutrinos have Dirac or pseudo-Dirac masses

manifesting the mixing between active neutrinos and heavy states. The resulting model consists of 3 light SM neutrino mass eigenstates ν_i ($i = 1, 2, 3$) and n heavier states, as introduced above. The flavor states will now consist of a combination of light and heavy states

$$\nu_\alpha = \sum_{i=1}^{3+n} U_{\alpha i} \nu_i, \quad (1.6)$$

and the leptonic part of the EW Lagrangian can be written as

$$\begin{aligned} \mathcal{L}_{EW}^\ell = & \frac{g}{\sqrt{2}} W_\mu^+ \sum_\alpha \sum_i U_{\alpha i}^* \bar{\nu}_i \gamma^\mu P_L \ell_\alpha + \frac{g}{4c_w} Z_\mu \\ & \times \left\{ \sum_{i,j} C_{ij} \bar{\nu}_i \gamma^\mu P_L \nu_j + \sum_\alpha \bar{\ell}_\alpha \gamma^\mu [2s_w^2 P_R - (1-2s_w^2) P_L] \ell_\alpha \right\} + \text{h.c.}, \end{aligned}$$

where $c_w \equiv \cos \theta_w$, $s_w \equiv \sin \theta_w$, and θ_w the SM weak mixing angle. P_L and P_R are the left and right projectors, respectively, while

$$C_{ij} \equiv \sum_\alpha U_{\alpha i}^* U_{\alpha j}. \quad (1.7)$$

The indices now sum over all $(3 + n)$ flavor and mass states.

Based on this formulation and assuming that only the mixing with the tau sector is open ($|U_{\alpha 4}^2| = 0$, $\alpha = e, \mu$), the relevant production diagram of the HNL can be drawn as shown in Figure 1.5. Alongside the fourth heavy mass state, a Hadronic cascade is produced. The heavy mass state will travel for some distance (dependent on mass and mixing) before it decays. The subsequent decay processes are depicted in Figure 1.6. It can be a CC or NC decay and both leptonic and mesonic modes are possible (dependent on the mass). This will produce a tau or a tau neutrino and another cascade that can be Electromagnetic or Hadronic. The branching ratios corresponding to the decay modes of the HNL for the mass range of interest (i.e. between 100 MeV and 1 GeV) are shown in Figure 1.7a as a function of the HNL mass.

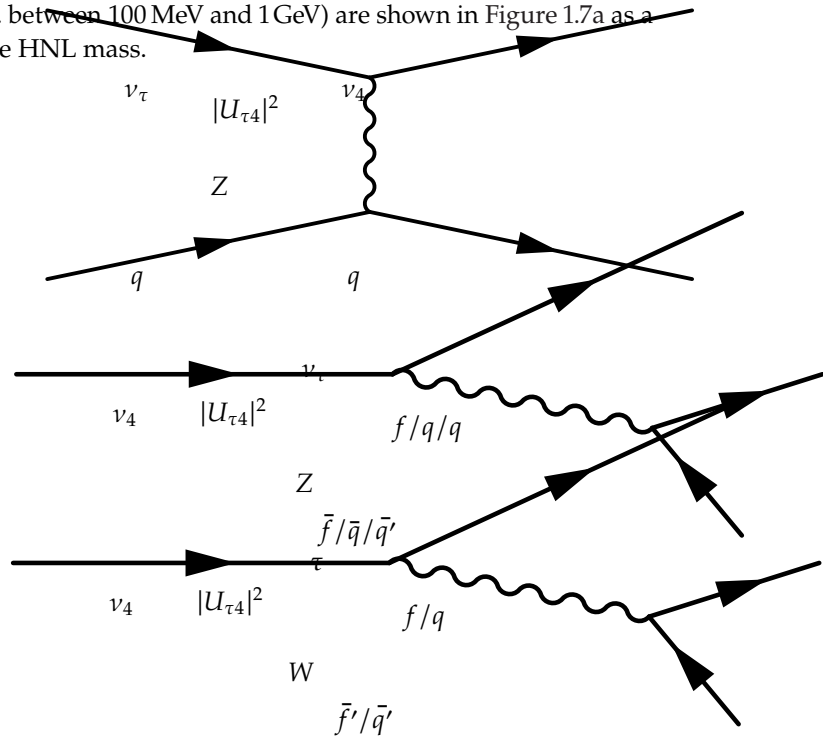


Figure 1.5: Production of a sterile neutrino in the up-scattering of a tau neutrino.

Figure 1.6: Sterile neutrino decay through neutral current (left) and charged current (right). With the current limits on $|U_{e4}|^2$ and $|U_{\mu 4}|^2$ being orders of magnitude stronger than that on $|U_{\tau 4}|^2$ [Atre:2009rg], the decay modes with an electron, an electron neutrino, a muon or a muon neutrino in the final state are not considered.

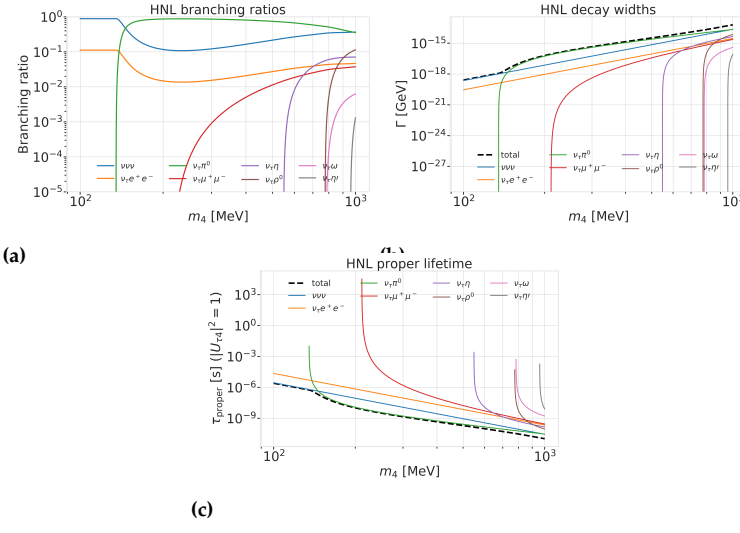


Figure 1.7: Branching ratios, decay widths, and proper lifetime of the HNL within the mass range considered, calculated based on the results from [14]. Given the existing constraints on $|U_{e4}|^2$ and $|U_{\mu 4}|^2$, we consider that the corresponding decay modes are negligible.

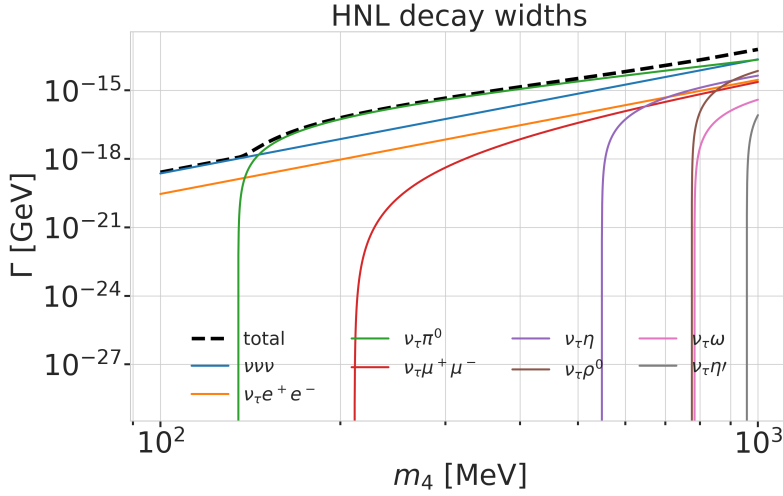


Figure 1.8: Decay widths of the HNL within the mass range considered, calculated based on the results from [14]. Given the existing constraints on $|U_{e4}|^2$ and $|U_{\mu 4}|^2$, we consider that the corresponding decay modes are negligible.

1.4.3 Production and Decay in IceCube DeepCore

1.4.4 Existing Constraints on Mixing

1.5 Neutrino Oscillations

1.5.1 Vacuum Oscillations

1.5.2 Oscillations in Matter

1.5.3 Atmospheric Neutrino Oscillations

(Re-)write BSM chapter for PhD thesis (just copy paste from M.Sc.).

[3]: Tanabashi et al. (2018), "Review of Particle Physics"

[15]: Honda et al. (2015), "Atmospheric neutrino flux calculation using the NRLMSISE-00 atmospheric model"

Neutrino Production in the Atmosphere

The flux of neutrinos used for this work exclusively comes from the Earth's atmosphere. When highly relativistic cosmic rays (protons and heavier nuclei [3]) interact in the upper atmosphere they produce a shower of particles. Neutrinos emerge from the decays of charged pions and kaons (π and K mesons) present in these showers. For energies below 100 GeV, the leading contribution comes from the pion decay chain

$$\begin{aligned} \pi^\pm &\rightarrow \mu^\pm + \nu_\mu(\bar{\nu}_\mu), \\ \mu^\pm &\rightarrow e^\pm + \bar{\nu}_\mu(\nu_\mu) + \nu_e(\bar{\nu}_e). \end{aligned} \quad (1.8)$$

The muons that also originate from this process are considered the main background source for IceCube. The left part of Figure 1.9 shows the atmospheric neutrino flux for the very broad energy spectrum in which they are produced. The flux expectations are calculated in the energy range of 100 MeV to 10 TeV for the South Pole [15], where the IceCube detector is located. From Equation 1.8 the ratio between muon and electron neutrinos can be inferred to be $N_{\nu_\mu} : N_{\nu_e} \approx 2 : 1$. This is only the case at muon energies below 1 GeV, where all muons decay in flight. For higher energies, muons can reach earth before decaying increasing the ratio to approximately 10:1 at around 100 GeV as shown in the right part of Figure 1.9. Additionally, kaon decays start to contribute which also increases the number of muons and muon neutrinos.

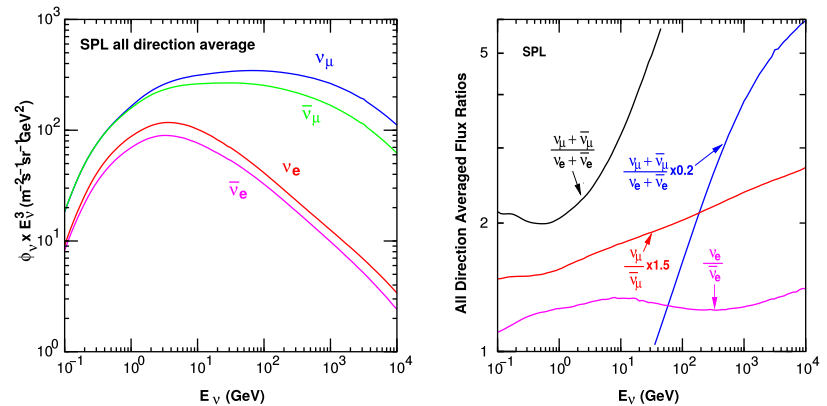


Figure 1.9: Atmospheric neutrino fluxes of the different flavors as a function of energy (left) and ratios between muon- and electron-neutrinos as well as ratios between neutrinos and antineutrinos for both flavors (right). Calculations are done for the geographic South Pole. Taken from [15].

[16]: Fedynitch et al. (2015), "Calculation of conventional and prompt lepton fluxes at very high energy"

SB: You could say why with an extra half-sentence.

[17]: Honda et al. (2007), "Calculation of atmospheric neutrino flux using the interaction model calibrated with atmospheric muon data"

In cosmic ray interactions, charged mesons or tau particles can also be produced, which leads to the formation of tau neutrinos. However, at the energy range considered for this work, the resulting tau neutrino flux is negligible as compared to the muon neutrino flux [16] and is not taken into account. It should be stated here that there is a rather large uncertainty on the normalization of the atmospheric neutrino flux on the order of 20-30 % [17] in the energy region of interest. This is mainly

due to uncertainties in the primary cosmic ray spectrum and modeling of the hadronic interactions.

Oscillations of Atmospheric Neutrinos

There are two ways to describe neutrino wave functions based on their Hamiltonian eigenvalues [18], as mass eigenstates or as flavor eigenstates. When applying a plane wave approach to explain the propagation of neutrinos in vacuum, their mass eigenstates evolve as

$$|\nu_k(t)\rangle = e^{-iE_k t/\hbar} |\nu_k\rangle, \quad (1.9)$$

where $E_k = \sqrt{\vec{p}^2 c^2 + m_k^2 c^4}$ is the energy of the mass eigenstate $|\nu_k\rangle$, with momentum \vec{p} and mass m_k . Alternatively, they can be described in terms of their flavor eigenstates, which relate the neutrinos to the charged leptons they interact with in weak CC interactions. The flavor eigenstates are ν_e , ν_μ , and ν_τ , whereas the mass eigenstates are called ν_1 , ν_2 , and ν_3 in the standard three-neutrino model. To understand the propagation of distinct neutrino flavors in time we need to relate the flavor eigenstates to the mass eigenstates. For massive neutrinos, each flavor eigenstate is a superposition of mass eigenstates [3]

$$|\nu_\alpha\rangle = \sum_k U_{\alpha k}^* |\nu_k\rangle, \quad (1.10)$$

where $|\nu_\alpha\rangle$ are the weak flavor states with $\alpha = e, \mu, \tau$ and $|\nu_k\rangle$ the mass states with $k = 1, 2, 3$. $U_{\alpha k}$ is the Pontecorvo-Maki-Nakagawa-Sakata (PMNS) matrix defining the mixing between mass and flavor eigenstates. The mixing matrix can be parameterized as [3]

$$U = \begin{pmatrix} 1 & 0 & 0 \\ 0 & c_{23} & s_{23} \\ 0 & -s_{23} & c_{23} \end{pmatrix} \begin{pmatrix} c_{13} & 0 & s_{13}e^{-i\delta_{CP}} \\ 0 & 1 & 0 \\ -s_{13}e^{i\delta_{CP}} & 0 & c_{13} \end{pmatrix} \begin{pmatrix} c_{12} & s_{12} & 0 \\ -s_{12} & c_{12} & 0 \\ 0 & 0 & 1 \end{pmatrix} \text{diag}(e^{i\rho_1}, e^{i\rho_2}, 1), \quad (1.11)$$

where $c_{ij} = \cos \theta_{ij}$ and $s_{ij} = \sin \theta_{ij}$ are cosine and sine of the mixing angle θ_{ij} , that defines the strength of the mixing between the mass eigenstates i and j and δ_{CP} is the neutrino CP-violating phase. Nonzero, non-equal neutrino masses and the neutrino mixing relation in Equation 1.10 lead to the observed phenomenon of neutrino oscillations. Oscillation means that a neutrino changes from its initial flavor to another flavor and back after traveling a certain distance. A produced flavor eigenstate $|\nu_\alpha\rangle$ propagates through space as a superposition of mass eigenstates. To find the probability that the initial flavor state $|\nu_\alpha\rangle$ ends up as the final flavor state $|\nu_\beta\rangle$ after the time t we calculate

$$P_{\nu_\alpha \rightarrow \nu_\beta}(t) = |\langle \nu_\beta | \nu_\alpha(t) | \nu_\beta | \nu_\alpha(t) \rangle|^2, \quad (1.12)$$

where P is the probability calculated by applying Fermi's Golden Rule [19]. Fermi's Golden Rule explains the transition rate from one energy eigenstate to another depending on the strength of the coupling between the two. The strength of the coupling is described by the square of the matrix element. Using the unitarity of the mixing matrix $U^{-1} = U^\dagger$ to reverse the relation Equation 1.10 and then time evolve the mass eigenstates with Equation 1.9 we get the time evolution of the flavor state

SB: I don't think this is true
- the normalization is known to 5% if you trust Anatoli/Juan Pablo. Please have a look at more recent publications on this topic.

[18]: Bilenky et al. (1978), "Lepton mixing and neutrino oscillations"

[3]: Tanabashi et al. (2018), "Review of Particle Physics"

[3]: Tanabashi et al. (2018), "Review of Particle Physics"

SB: formatting/margins also
I don't think you defined
rho1,2

[19]: Dirac (1927), "The Quantum Theory of the Emission and Absorption of Radiation"

$|\nu_\alpha(t)\rangle$. Inserting this result into Equation 1.12 yields

$$P_{\nu_\alpha \rightarrow \nu_\beta}(t) = \sum_{j,k} U_{\beta j}^* U_{\alpha j} U_{\beta k} U_{\alpha k}^* e^{-i(E_k - E_j)t/\hbar}, \quad (1.13)$$

where the indices j and k run over the mass eigenstates. For small neutrino masses compared to their kinetic energy, we can approximate the energy as

$$E_k \approx E + \frac{c^4 m_k^2}{2E} \quad \rightarrow \quad E_k - E_j \approx \frac{c^4 \Delta m_{kj}^2}{2E}, \quad (1.14)$$

where $\Delta m_{kj}^2 = m_k^2 - m_j^2$ is the mass-squared splitting between states k and j . If we now replace the time in Equation 1.13 by the distance traveled by the relativistic neutrinos $t \approx L/c$ we get

$$\begin{aligned} P_{\nu_\alpha \rightarrow \nu_\beta}(t) &= \delta_{\alpha\beta} - 4 \sum_{j>k} \text{Re}(U_{\beta j}^* U_{\alpha j} U_{\beta k} U_{\alpha k}^*) \sin^2\left(\frac{c^3 \Delta m_{kj}^2}{4E\hbar} L\right) \\ &\quad + 2 \sum_{j>k} \text{Im}(U_{\beta j}^* U_{\alpha j} U_{\beta k} U_{\alpha k}^*) \sin^2\left(\frac{c^3 \Delta m_{kj}^2}{4E\hbar} L\right), \end{aligned} \quad (1.15)$$

which is referred to as the survival probability if $\alpha = \beta$ and the transition probability if $\alpha \neq \beta$. The probability in Equation 1.15 is only nonzero if there are neutrino mass eigenstates with masses greater than zero. Additionally, there must be a mass-squared difference Δm^2 and nonzero mixing between the states. Since we assumed propagation in vacuum in Equation 1.9, the transition and survival probabilities correspond to vacuum mixing.

Matter Effects

1.6 Open Questions in Neutrino Particle Physics

Heavy Neutral Lepton Signal Simulation

2

After the SM simulation generation and the default low energy event selection and processing chain were introduced in the previous Chapter ??, the focus will now be on the central part of this thesis - the HNL signal simulation. Since this is the first attempt of performing a search for HNLs with IceCube DeepCore, there was no prior knowledge of the expected performance nor the event expectation, and the simulation had to be developed from scratch. Two avenues of simulation generation were pursued in parallel; a collection of model independent simulation sets was realized and is explained in Section 2.1 and the physically accurate model dependent simulation is described in Section 2.2.

| | | |
|-----|------------------------------|----|
| 2.1 | Model Independent Simulation | 11 |
| 2.2 | Model Dependent Simulation | 15 |

2.1 Model Independent Simulation

To investigate the potential of IceCube to detect HNLs by identifying the unique double cascade morphology explained in Section 1.4.3, it is very valuable to have simulation sets where the double cascade kinematics can be controlled directly. In a realistic model the decay kinematics and the absolute event expectation all depend on the specific model parameters chosen (see Section 1.4). To decouple the simulation from a specific parameter choice, a model independent double cascade generator was developed and will be explained in the following sections. Based on the generator a few simulation sets were produced to investigate the performance of IceCube DeepCore to detect low energetic double cascades, dependent on their properties. The results of this study will be discussed in Chapter 3.

2.1.1 Generator Functions

In order to produce the model independent simulation sets a series of generator functions was implemented in PYTHON [20]. The collection of functions can be found in [this public repository](#). A few independent functions are needed to perform the sampling based on a random variable between 0 and 1 as input. There is a simple function to return a random sign (+1/-1) and two functions to sample from a power law and an exponential distribution. The inputs are the wanted sampling range and the power law index or the exponential decay constant, respectively. They both apply the inverse transformation method.

[20]: Van Rossum et al. (2009), *Python 3 Reference Manual*

Additionally, there are some functions that are IceCube specific. Two functions are implemented to transform a direction from IceCube zenith/azimuth angles to a direction vector and vice versa. There is a function to create an EM cascade particle from position, direction, energy, and time and another to produce an arbitrary list of EM cascades, with the previous function, given the list of input parameters, and then adding it to the current IceCube event. Based on these functions, any specific simulation set can be produced by choosing the sampling distributions

and number of cascades to be placed in each event and then calling the generator functions with the input parameters based on these sampling distributions.

IceCube software framework

The functions described above are based on the ([public](#)) `icetray` software project and the EM particles are defined as type `I3Particle`, while the object to store the MC particles is called `I3MCTree` and each IceCube event information is in one `I3Frame` object.

2.1.2 Simplistic Sets

To test the implemented generator functions and investigate some idealistic double cascade event scenarios, two sets are produced for straight up-going events that are centered on a string and horizontal events located inside DeepCore.

Make my own DC string positions/distances plot version.

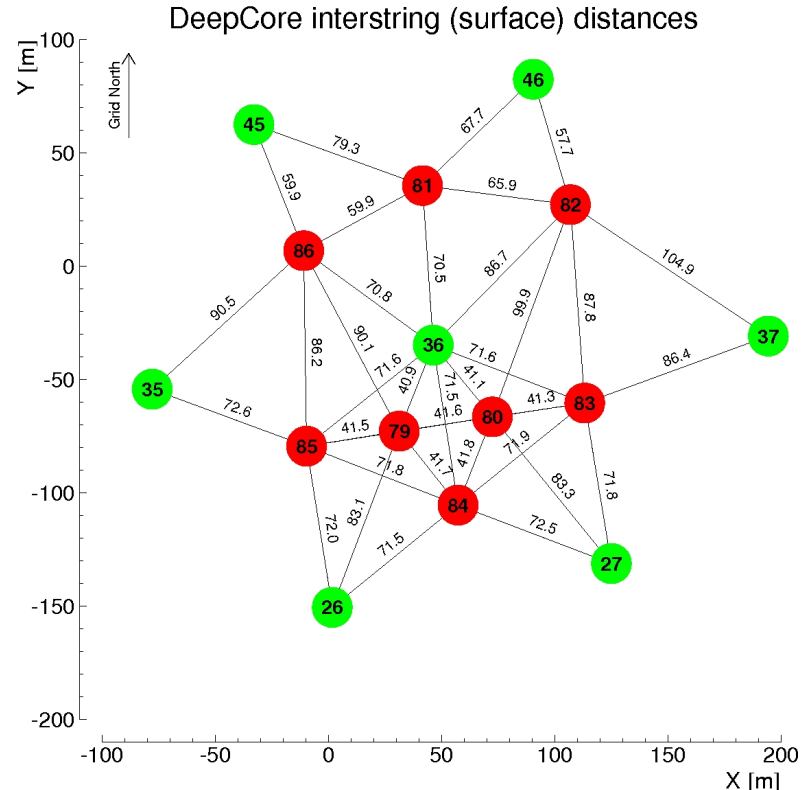


Figure 2.1: Horizontal positions and distances between DeepCore strings. Red strings are instrumented more densely (vertically) and partially have higher quantum efficiency (HQE) DOMs.

The first set is used to investigate one of the potentially best possible cases to detect a double cascade where both cascades are placed on a DeepCore string (namely string 81) and the directions are directly up-going. The horizontal positions and distances of all DeepCore fiducial volume strings are shown in Figure 2.1 and string 81 is at a medium distance of ~ 70 m to its neighboring strings. As already mentioned in Section ??, DeepCore strings have higher quantum efficiency DOMs and a denser vertical spacing, making them better to detect low energetic events that produce little light. To produce the events, the x, y position of the cascades is fixed to the center of string 81 while the z position is

| Set | Variable | Distribution | Range/Value |
|-------------------|---------------|------------------|--------------------------------|
| Up-going | | | |
| | energy | uniform | 0.0 GeV to 60.0 GeV |
| | zenith | fixed | 180.0° |
| | azimuth | fixed | 0.0° |
| | x, y position | fixed | (41.6, 35.49) m |
| | z position | uniform | -480.0 m to -180.0 m |
| Horizontal | | | |
| | energy | uniform | 0.0 GeV to 60.0 GeV |
| | zenith | fixed | 90.0° |
| | azimuth | uniform | 0.0° to 360.0° |
| | x, y position | uniform (circle) | c=(46.29, -34.88) m, r=150.0 m |
| | z position | fixed | -330.0 m |

Table 2.1: Generation level sampling distributions and ranges/values of up-going and horizontal model independent simulation.

sampled uniformly along the strings z elongation and the energies are sampled uniformly between 0.0 GeV and 60.0 GeV. The specific sampling distributions/values for the cascades are listed in Table 2.1. The order of the cascades is chosen such that the lower one is first ($t_0 = 0.0$ ns) and the upper one is second ($t_1 = L/c$), assuming the speed of light c as speed of the heavy mass state, traveling between the two cascades.

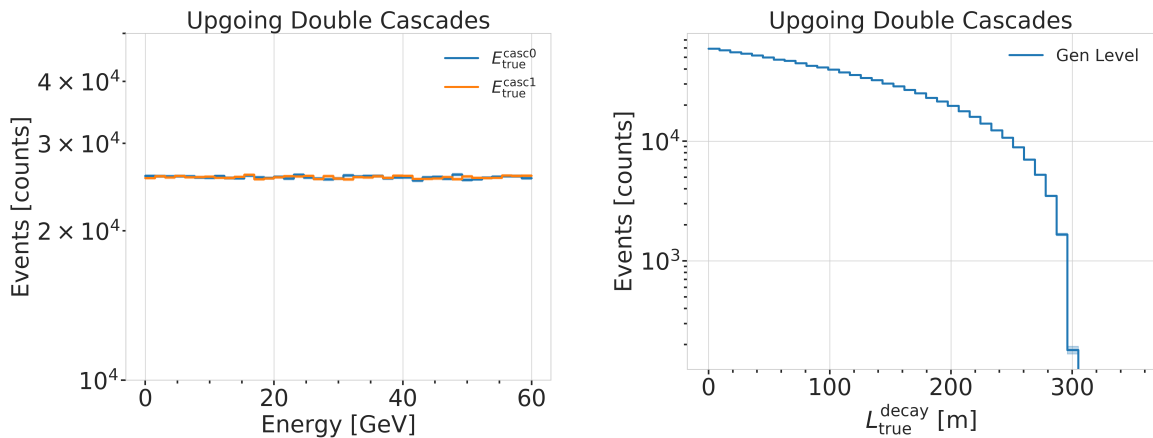


Figure 2.2: Generation level distributions of the simplistic simulation sets. Cascade and total energies (left) and decay lengths (right) of both sets are shown.

The second set is used to investigate the reconstruction performance for horizontal events, where the spacing between DOMs is much larger. The cascades are placed uniformly on a circle centered in DeepCore. The direction is always horizontal and azimuth is defined by the connecting vector of both cascade positions. The energies are again sampled uniformly between 0.0 GeV and 60.0 GeV and the detailed sampling distributions/values are also listed in Table 2.1. Some examples of the generation level distributions of the simplified sets are shown in Figure 2.2, while further distributions can be found in Figure ???. The variables that are uniformly sampled or fixed to a certain value are not presented.

Re-make plot with all energies (cascades and total, both sets (they are the same))

Re-make plot with all decay lengths (both sets)

2.1.3 Realistic Set

To thoroughly investigate the potential of IceCube DeepCore to detect double cascade events, a more realistic simulation set is produced that aims to be as close as possible to the expected signal simulation explained

Table 2.2: Generation level sampling distributions and ranges/values of the realistic model independent simulation.

| Variable | Distribution | Range/Value |
|----------------------|--------------------------|----------------------------------|
| energy (total) | power law E^{-2} | 1 GeV to 1000 GeV |
| decay length | exponential $e^{-0.01L}$ | 0 m to 1000 m |
| zenith | uniform | 70° to 180° |
| azimuth | uniform | 0° to 360° |
| x, y (one cascade) | uniform (circle) | $c=(46.29, -34.88)$ m, $r=150$ m |
| z (one cascade) | uniform | -480.0 m to -180.0 m |

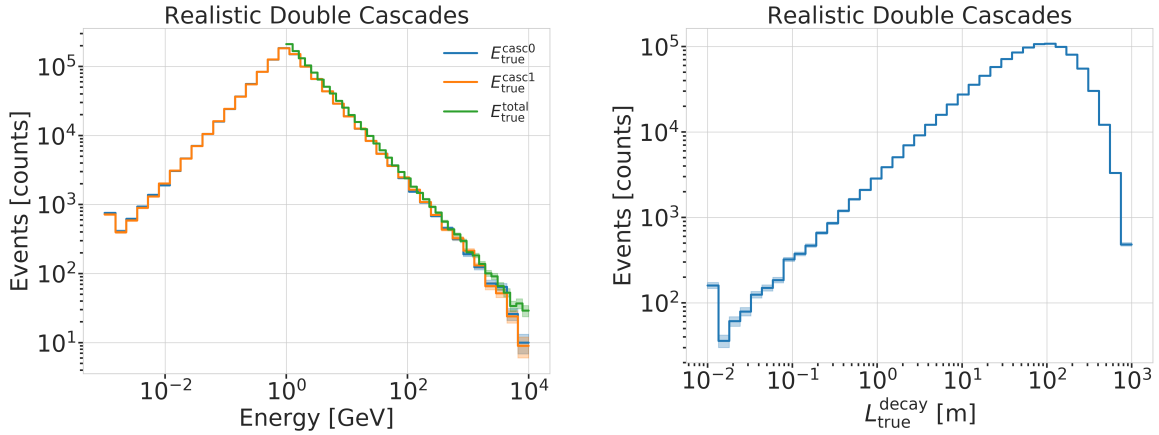


Figure 2.3: Generation level distributions of the simplistic realistic set. Shown are the cascade and total energies (left) and decay lengths (right).

in Section 2.2, while still allowing some freedom to control the double cascade kinematics. For this purpose the total energy is sampled from an E^{-2} power law, mimicking the energy spectrum of the primary neutrinos as stated in Section ???. Although in the realistic process described in Section 2.2 the energy is distributed in a more complex way into the two cascades and secondary particles, it is a good approximation to simply divide the total energy into two parts. This is done by randomly assigning a fraction between 0 % and 100 % to one cascade and the remaining part to the other cascade. In this way the whole sample covers various cases of energy distributions between the two cascades. To efficiently generate events in a way that produces distributions similar to what would be observed with DeepCore, one of the cascade positions is sampled inside the DeepCore volume by choosing its coordinates randomly on a cylinder that is centered in DeepCore. This is similar to a trigger condition of one cascade always being inside the DeepCore fiducial volume. By choosing the direction of the event sampling zenith and azimuth uniformly between 70° and 180° and 0° and 360°, respectively, the position of the other cascade can be inferred for a given decay length. The length is sampled from an exponential distribution, which would be expected for the decaying heavy mass state. Based on the direction and the decay length, the position of the other cascade is found, assuming a travel speed of c and randomly choosing whether the cascade position that was sampled is the first cascade or the second and then assigning the other cascade position accordingly. The sampling distributions/values are listed in Table 2.4. Example distributions of the generation level variables are shown in Figure 2.3, while further distributions can be found in Figure ??.

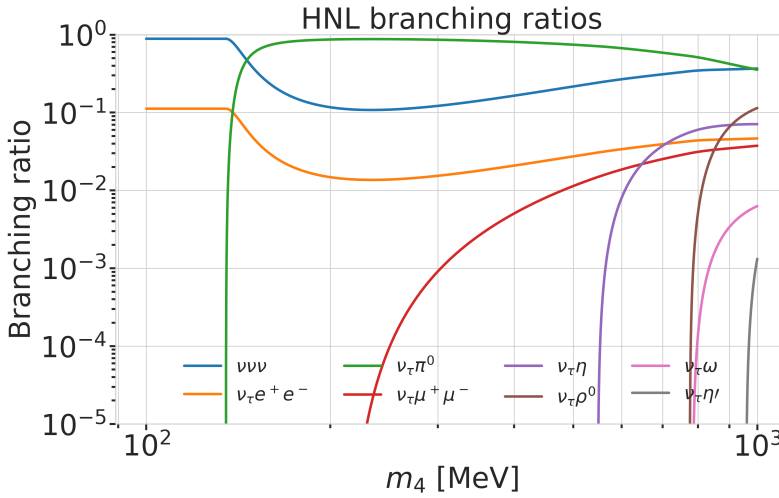
2.2 Model Dependent Simulation

To get a realistic estimate of the HNL event expectation in IceCube DeepCore, depending on the specific model parameters, a generator was developed that is based on the HNL theory introduced in Section 1.4. For this work, only the interaction with the τ -sector was taken into account ($|U_{\alpha 4}^2| = 0, \alpha = e, \mu$), which reduces the physics parameters of interest and relevant for the simulation to the fourth heavy lepton mass, m_4 , and the mixing, $|U_{\tau 4}^2|$. The generator uses a customized *LeptonInjector* (LI) version to create the events and *LeptonWeighter* (LW) to weight them [21]. The modified LI and the essential components needed for the HNL simulation are described in the next sections, followed by the description of the weighting scheme and the sampling distributions chosen for the simulation generation.

[21]: Abbasi et al. (2021), “LeptonInjector and LeptonWeighter: A neutrino event generator and weighter for neutrino observatories”

2.2.1 Custom LeptonInjector

In its standard version, the LI generator produces neutrino interactions by injecting a lepton and a cascade¹ at the interaction vertex of the neutrino, where the lepton is the charged (neutral) particle produced in a CC (NC) interaction and the cascade is the hadronic cascade from the breaking nucleus. Both objects are injected with the same (x, y, z, t) coordinates and the kinematics are sampled from the differential and total cross-sections that are one of the inputs to LI.



1: The cascades are defined as icetray I3Particles with type *Hadrons*.

Figure 2.4: Branching ratios of the HNL within the mass range considered in this work, only considering $|U_{\tau 4}^2| \neq 0$, calculated based on the results from [14].

In the modified version, the lepton at the interaction vertex is replaced by the HNL, where the interaction cross-sections are replaced by custom, mass dependent HNL cross-sections. The HNL is forced to decay after a chosen distance to produce secondary SM particles, where the decay mode is randomly chosen based on the mass dependent branching ratios from the kinematically accessible decay modes shown in Figure 2.4. The cross-section and decay width calculations were implemented for this purpose and will be explained in more detail in the following. Another needed addition to LI is that the decay products of the HNL are also added to the list of MC particles in each event. They are injected with the correctly displaced position and delayed time from the interaction vertex, given the HNL decay length. These HNL daughter particles form

[22]: Alwall et al. (2014), “The automated computation of tree-level and next-to-leading order differential cross sections, and their matching to parton shower simulations”

[24]: Levy (2009), “Cross-section and polarization of neutrino-produced tau’s made simple”

the second cascade, not as a single cascade object, but as the explicit particles forming the shower. The kinematics of the two-body decays are computed analytically, while the three-body decay kinematics are calculated with `MADGRAPH` [22], which will also be explained further below. Independent of the number of particles in the final state of the HNL decay, the kinematics are calculated/simulated at rest and then boosted along the HNL momentum.

Any number of files can be produced, where the number of events per file is also variable. The injection is done using the *LI volume mode*, for the injection of the primary particle on a cylindrical volume, adding 50 % of the events with ν_τ and the other half with $\bar{\nu}_\tau$ as primary particle type. The generator takes the custom double-differential/total cross-section splines described below and the parameters defining the sampling distributions as inputs.

Cross-Sections

The cross-sections are calculated using the `NuXSSplMkr` [23] software, which is a tool to calculate neutrino cross-sections from *parton distribution functions (PDFs)* and then produce splines that can be read and used with `LI/LW`. The tool was customized to produce the custom HNL cross-sections, where the main modification to calculate the cross-sections for the ν_τ -NC interaction into the new heavy mass state is the addition of a kinematic condition to ensure that there is sufficient energy to produce the heavy mass state. It is the same condition that needs to be fulfilled for the CC case, where the outgoing charged lepton mass is non-zero. Following [24] (equation 7), the condition

$$(1 + x\delta_N)h^2 - (x + \delta_4)h + x\delta_4 \leq 0 \quad (2.1)$$

is implemented for the NC case in the `NuXSSplMkr` code. Here $\delta_4 = \frac{m_4^2}{s-M^2}$, $\delta_N = \frac{M^2}{s-M^2}$, and $h \stackrel{\text{def}}{=} xy + \delta_4$, with x, y being the Bjorken variables, m_4 and M the mass of the heavy state and the target nucleon, respectively, and s the center of mass energy squared.

Re-make plot with 3 target masses and better labels

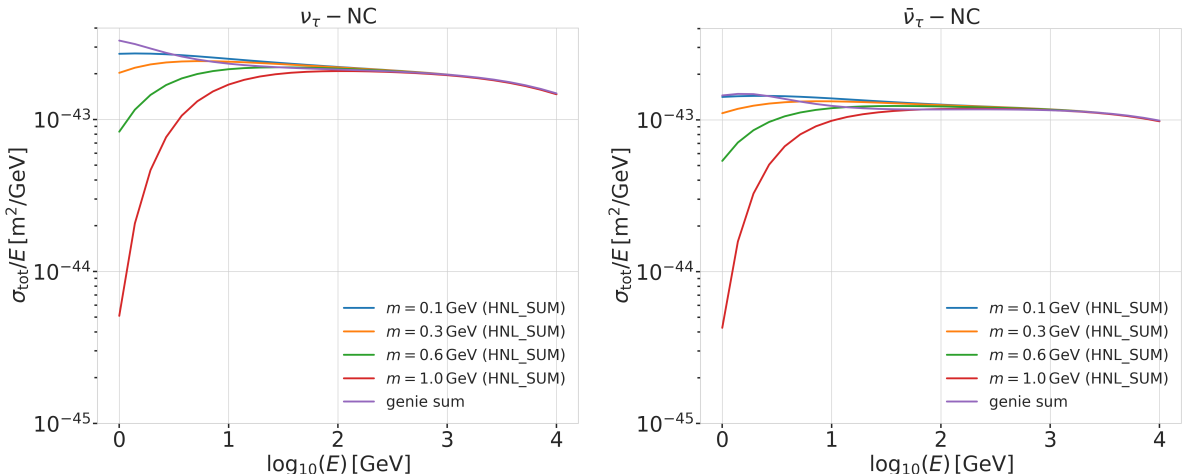


Figure 2.5: Custom HNL total cross-sections for the four target masses compared to the total ($\nu_\tau/\bar{\nu}_\tau$ NC) cross-section used for SM neutrino simulation production with GENIE.

As already described in Section ??, the SM neutrino background simulation is created using the GRV98LO PDFs. These PDFs also had to be added to the cross-section spline maker, to ensure good agreement between the background and signal cross-sections. The double differential ($ds/dx dy$) and total (σ) cross-sections were produced for the chosen target HNL masses and then splined. The produced cross-section are added to the custom LI version and used for the simulation generation and weighting. Figure 2.5 shows the total cross-sections that were produced compared to the cross-section used for the production of the SM $\nu_\tau/\bar{\nu}_\tau$ NC background simulation. Above $\sim 2 \times 10^2$ GeV they match, which is the wanted result of using the identical input PDFs.

Decay Channels

The accessible decay channels are dependent on the mass of the HNL and the allowed mixing. For this analysis, where only $|U_{\tau 4}|^2 \neq 0$, the considered decay channels are listed in Table 2.3 and the corresponding branching ratios are shown in Figure 2.4. The individual branching ratio for a specific mass is calculated as $BR_i(m_4) = \Gamma_i(m_4)/\Gamma_{\text{total}}(m_4)$, where $\Gamma_{\text{total}}(m_4) = \sum \Gamma_i(m_4)$. The formulas to calculate the decay widths show up in multiple references, but we chose to match them to [14], which also discusses the discrepancies in previous literature.

2-Body Decay Widths The decay to a neutral pseudoscalar meson is

$$\Gamma_{\nu_4 \rightarrow \nu_\tau P} = |U_{\tau 4}|^2 \frac{G_F^2 m_4^3}{32\pi} f_P^2 (1 - x_p^2)^2, \quad (2.2)$$

with $x_P = m_P/m_4$ and

$$f_{\pi^0} = 0.130 \text{ GeV}, \quad f_\eta = 0.0816 \text{ GeV}, \quad C_2 = f_{\eta'} = -0.0946 \text{ GeV}, \quad (2.3)$$

while the decay to a neutral vector meson is given by

$$\Gamma_{\nu_4 \rightarrow \nu_\tau V} = |U_{\tau 4}|^2 \frac{G_F^2 m_4^3}{32\pi} \left(\frac{f_V}{m_V} \right)^2 g_V^2 (1 + 2x_V^2)(1 - x_V^2)^2, \quad (2.4)$$

with $x_V = m_V/m_4$,

$$f_{\rho^0} = 0.171 \text{ GeV}^2, \quad f_\omega = 0.155 \text{ GeV}^2, \quad (2.5)$$

and

$$g_{\rho^0} = 1 - 2 \sin^2 \theta_w, \quad g_\omega = \frac{-2 \sin^2 \theta_w}{3}, \quad \sin^2 \theta_w = 0.2229 \quad (2.6)$$

[25].

3-Body Decay Widths The (invisible) decay to three neutrinos is

$$\Gamma_{\nu_4 \rightarrow \nu_\tau \nu_\alpha \bar{\nu}_\alpha} = |U_{\tau 4}|^2 \frac{G_F^2 m_4^5}{192\pi^3}, \quad (2.7)$$

Add comparisons of SM cross-sections between NuXSSplMkr and genie?

add varied total cross-section for a few background HNL events (for QE/RES variations?!)

[14]: Coloma et al. (2021), "GeV-scale neutrinos: interactions with mesons and DUNE sensitivity"

| Channel | Opens | $\hat{BR} [\%]$ |
|--|---------|-----------------|
| $\nu_4 \rightarrow \nu_\tau \nu_\alpha \bar{\nu}_\alpha$ | 0 MeV | 100.0 |
| $\nu_4 \rightarrow \nu_\tau e^+ e^-$ | 1 MeV | ? |
| $\nu_4 \rightarrow \nu_\tau \pi^0$ | 135 MeV | ? |
| $\nu_4 \rightarrow \nu_\tau \mu^+ \mu^-$ | 211 MeV | ? |
| $\nu_4 \rightarrow \nu_\tau \eta$ | 548 MeV | ? |
| $\nu_4 \rightarrow \nu_\tau \rho^0$ | 770 MeV | ? |
| $\nu_4 \rightarrow \nu_\tau \omega$ | 783 MeV | ? |
| $\nu_4 \rightarrow \nu_\tau \eta'$ | 958 MeV | ? |

Table 2.3: Possible decay channels of the HNL, considering only $|U_{\tau 4}|^2 \neq 0$. Listed is the mass at which each channel opens and the maximum branching ratio.

Calculate max BRs

[25]: Tiesinga et al. (2021), "CODATA recommended values of the fundamental physical constants: 2018"

while the decay to two charged leptons (using $x_\alpha = (m_\alpha/m_4)^2$) of the same flavor reads

$$\Gamma_{\nu_4 \rightarrow \nu_\tau l_\alpha^+ l_\alpha^-} = |U_{\tau 4}|^2 \frac{G_F^2 m_4^5}{192\pi^3} [C_1 f_1(x_\alpha) + C_2 f_2(x_\alpha)], \quad (2.8)$$

with the constants defined as

$$C_1 = \frac{1}{4}(1 - 4s_w^2 + 8s_w^4), \quad C_2 = \frac{1}{2}(-s_w^2 + 2s_w^4), \quad (2.9)$$

the functions as

$$f_1(x_\alpha) = (1 - 14x_\alpha - 2x_\alpha^2 - 12x_\alpha^3)\sqrt{1 - 4x_\alpha} + 12x_\alpha^2(x_\alpha^2 - 1)L(x_\alpha), \quad (2.10)$$

$$f_2(x_\alpha) = 4[x_\alpha(2 + 10x_\alpha - 12x_\alpha^2)\sqrt{1 - 4x_\alpha} + 6x_\alpha^2(1 - 2x_\alpha + 2x_\alpha^2)L(x_\alpha)], \quad (2.11)$$

and

$$L(x) = \ln\left(\frac{1 - 3x - (1 - x)\sqrt{1 - 4x}}{x(1 + \sqrt{1 - 4x})}\right). \quad (2.12)$$

MadGraph 3-Body Decays

[14]: Coloma et al. (2021), “GeV-scale neutrinos: interactions with mesons and DUNE sensitivity”

The specific MadGraph version used to produce the 3-body decay kinematics is [MadGraph4 v3.4.0](#). As input, the decay diagrams calculated with [FeynRules 2.0](#) using the Lagrangians derived in [14] are taken. The Universal FeynRules Output (UFO) from `EFFECTIVE_HEAVY_N_MAJORANA_-v103` were used for our calculation. For each mass and corresponding decay channels, we produce 1×10^6 decay kinematic variations in the rest frame and store those in a text file. During event generation, we randomly pick an event from that list, to simulate the decay kinematics of a 3-body decay.

2.2.2 Sampling Distributions

In principle, the generation level sampling distributions should be chosen such that at final level of the selection chain, the for the analysis relevant phase space is covered with sufficient statistics to make a reasonable estimate of the event expectation. Insufficiently large initial distributions lead to an underestimate of the expected rates, which is still correct as in being the more conservative estimate, but limiting the analysis potential. Three discrete simulation sets were produced with HNL masses of 0.3 GeV, 0.6 GeV and 1.0 GeV. Each set consist of a part that is generated for very short decay lengths and one for long decay lengths, because during development it became clear that the low lengths component is crucial to get a reasonable event estimate. To remaining sampling distributions are identical for all sets and are listed in Table ???. The target file number for each set was 5000, with 5×10^5 events per file.

| Variable | Distribution | Range/Value |
|--------------------|------------------------------|------------------------------|
| energy | E^{-2} | [2 GeV, 1×10^4 GeV] |
| zenith | uniform (in $\cos(\theta)$) | [80°, 180°] |
| azimuth | uniform | [0°, 360°] |
| vertex x, y | uniform | $r=600$ m |
| vertex z | uniform | -600 m to 0 m |
| m_4 | fixed | [0.3, 0.6, 1.0] GeV |
| L_{decay} | L^{-1} | [0.0004, 1] m / [1, 1000] m |

Table 2.4: Generation level sampling distributions and ranges/values of the model dependent simulation sets.

2.2.3 Weighting Scheme

To produce physically correct event distributions based on the arbitrary generation sampling distributions for the HNL simulation, the forward folding method that was already introduced for the SM simulation in Section ?? is used again. How this will be applied in the analysis is discussed in Section 4.2. The weighting scheme that will be explained in the following is implemented in the IceCube low energy analysis framework PISA in [this custom stage](#). The only needed input is the mixing strength $|U_{\tau 4}|^2$, which is the variable physics parameter in this analysis. This weighting is needed to go from the used decay length sampling distribution (inverse $1/L$ with fixed range in lab frame) to the target distribution (exponential defined by proper lifetime of the HNL). For each event the additional weight is calculated using the gamma factor

$$\gamma = \frac{\sqrt{E_{\text{kin}}^2 + m_4^2}}{m_4}, \quad (2.13)$$

with the HNL mass m_4 and it's kinetic energy E_{kin} . The speed of the HNL is calculated as

$$v = c \cdot \sqrt{1 - \frac{1}{\gamma^2}}, \quad (2.14)$$

where c is the speed of light. With these the lab frame decay length range $[s_{\min}, s_{\max}]$ can be converted into the rest frame lifetime range $[\tau_{\min}, \tau_{\max}]$ for each event

$$\tau_{\min/\max} = \frac{s_{\min/\max}}{v \cdot \gamma}. \quad (2.15)$$

The proper lifetime of each HNL event can be calculated using the total decay width Γ_{total} from Section 1 and the chosen mixing strength $|U_{\tau 4}|^2$ as

$$\tau_{\text{proper}} = \frac{\hbar}{\Gamma_{\text{total}}(m_4) \cdot |U_{\tau 4}|^2}, \quad (2.16)$$

where \hbar is the reduced Planck constant. Since the decay lengths/lifetimes of the events are sampled from an inverse distribution instead of an exponential as it would be expected from a particle decay we have to re-weight accordingly to achieve the correct decay length/lifetime distribution. This is done by using the wanted exponential distribution

$$\text{PDF}_{\text{exp}} = \frac{1}{\tau_{\text{proper}}} \cdot e^{\frac{-\tau}{\tau_{\text{proper}}}}, \quad (2.17)$$

and the inverse distribution that was sampled from

$$\text{PDF}_{\text{inv}} = \frac{1}{\tau \cdot (\ln(\tau_{\max}) - \ln(\tau_{\min}))}. \quad (2.18)$$

where is PISA introduced? is there a reference?

This re-weighting factor is then calculated as

$$w_{\text{lifetime}} = \frac{\text{PDF}_{\text{exp}}}{\text{PDF}_{\text{inv}}} = \frac{\Gamma_{\text{total}}(m_4) \cdot |U_{\tau 4}|^2}{\hbar} \cdot \tau \cdot (\ln(\tau_{\max}) - \ln(\tau_{\min})) \cdot e^{\frac{-\tau}{\tau_{\text{proper}}}}. \quad (2.19)$$

Adding another factor of $|U_{\tau 4}|^2$ to account for the mixing at the interaction vertex the total re-weighting factor becomes

$$w_{\text{total}} = |U_{\tau 4}|^2 \cdot w_{\text{lifetime}}. \quad (2.20)$$

add table with number of gen level files? mention the event number is smaller because of kinematic condition?

If this additional weighting factor is multiplied to a generation weight (like in Equation ??), the livetime, and the oscillated primary neutrino flux, it results in the number of expected events in the detector for this particular MC event for a chosen mixing (and mass).

2.2.4 Generation Level Distributions

Figure 2.6 shows some selected generation level distributions. Additional distributions can be found in Figure ??.

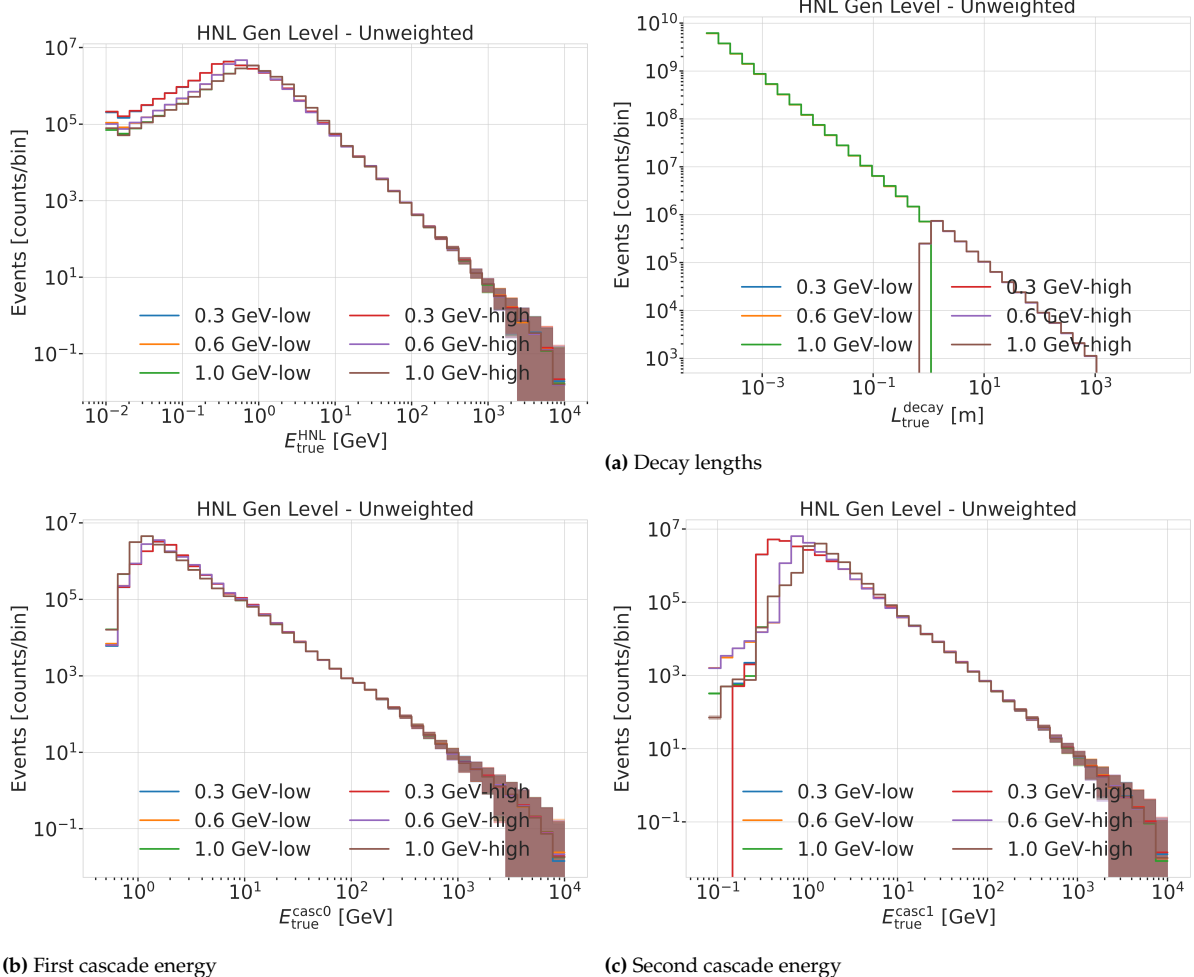


Figure 2.6: Generation level distributions of the model dependent simulation.

Detecting Low Energetic Double Cascades

3

3.1 Reconstruction

3.1.1 Table-Based Minimum Likelihood Algorithms

| | | |
|-----|----------------|----|
| 3.1 | Reconstruction | 21 |
| 3.2 | Cross Checks | 21 |
| 3.3 | Performance | 22 |

3.1.2 Double Cascade Hypothesis

3.1.3 Modification to Low Energy Events

3.2 Cross Checks

3.2.1 Simplistic Sets

After generation the events are processed with standard Photon, Detector, L1, and L2 processing and then Taupede+MuMillipede is run on top of the L2 files. Multiple versions with different parameters were produced, some with the OscNext baseline parameters, some without detector noise (in Det level) and some with h2-50cm holeice model, to match the holeice model that was used to generate the photonics tables.

BrightDom Cleaning To investigate the effect of the BrightDom cleaning cut the 194601 set without detector noise (and baseline hole ice model) is used. The BrightDom cleaning is needed to stop a few DOMs with many photon hits to drive the reconstruction because this leads to large biases in the energy estimations. Historically, the BrightDom cleaning was removing all DOMs that had a charge larger than 10 times the mean charge. After quickly checking some charge distributions and how the mean behaves it was clear that the cut should better be defined based on a metric that is less affected by outliers, like the median. Figure ?? shows where the mean and the median are located for an example event. The cut was re-defined to use the median instead of the mean and 10% of the simulation were processed with [Taupede](#) using 30x and 100x the median as BrightDom cutoff. Figure ?? shows where these values fall for the same example event.

As a quick check of the performance of both cuts the decay length resolution/bias and the resolutions/biases of all energies were checked. The reconstructed decay length is almost not affected by applying this cut, which is as expected, because it is mostly dependent on the arrival time of the photons. The effect on the reconstructed energy is much stronger, where a looser cut (100x) shows a significantly larger bias than the tighter cut at (30x). Even though this was not a highly sophisticated optimization of the BrightDom cut, an improvement was achieved by changing from mean to median and selecting the tighter cut (of the two tested). It's hard to tell how this would perform for high energy events, but I'm quite certain that a definition based on the median would be more reliable than on the mean.

3.3 Performance

3.3.1 Energy/Decay Length Resolution

3.3.2 Double Cascade Classification

Search for an Excess of Heavy Neutral Lepton Events

4

The measurement performed in this thesis is the search for an excess of HNL events in the 10 years of IceCube DeepCore data. In principle the two physics parameters to be probed are the mass of the HNL, m_4 , and the mixing between the fourth heavy mass state and the SM τ sector, $|U_{\tau 4}|^2$. Since the mass itself influences the production and decay kinematics of the event and the accessible decay modes, individual mass sets were produced as described in Section 2.2. The mass slightly influences the energy distribution, while the mixing both changes the overall scale of the HNL events and the shape in energy and PID. IceCube DeepCore is suited to measure the excess which appears around and below 20 GeV, due to its production from the atmospheric tau neutrinos, although a reduced lower energy threshold could improve the analysis. The measurement will be performed for the three mass sets individually, while the mixing is the parameter that can be varied continuously and will be measured in the fit.

4.1 Final Level Sample

The final level sample of this analysis always consists of the neutrino and muon MC introduced in Section ?? and one of the three HNL samples explained in Section 2.2. All of those simulation sets and the 10 years of IceCube DeepCore data are processed through the full processing and event selection chain described in Section ?? leading to the final level sample. Since applying the last cuts from Section ?? leaves an insignificant amount of pure noise events in the sample, the noise simulation is not included in the analysis and won't be listed here.

4.1.1 Expected Rates/Events

The rates and the expected events in 10 years are shown in Table 4.1. For the HNL the expectation depends on the mass and the mixing. Shown here are two example mixings for all the three masses. A mixing of 0.0 would result in a rate of 0.0 and therefore no HNL events.

| Type | Rate [mHz] | Events (in 10 years) | |
|------------------------|------------|----------------------------|----------------------------|
| ν_μ^{CC} | 0.3522 | 103063 ± 113 | |
| ν_e^{CC} | 0.1411 | 41299 ± 69 | |
| ν_τ^{CC} | 0.0348 | 10187 ± 22 | |
| ν_{NC} | 0.0667 | 968 ± 57 | |
| μ | 0.0033 | 19522 ± 47 | |
| HNL | | $ U_{\tau 4} ^2 = 10^{-3}$ | $ U_{\tau 4} ^2 = 10^{-1}$ |
| $m_4=0.3 \text{ GeV}$ | x.xxx | 2.5 | 1342.5 |
| $m_4=0.6 \text{ GeV}$ | x.xxx | 9.0 | 1207.0 |
| $m_4=1.0 \text{ GeV}$ | x.xxx | 9.6 | 966.5 |

| | |
|------------------------------------|----|
| 4.1 Final Level Sample | 23 |
| 4.2 Statistical Analysis | 24 |
| 4.3 Analysis Checks | 25 |
| 4.4 Results | 26 |

add information about the matter profile used

add information about the oscillation probability calculation and the software used for it

get correct final level rates from my pipeline(s)

add rate and Poisson error for HNL samples

maybe just pick one mixing?

Table 4.1: Final level rates and event expectation of the SM background particle types and the HNL signal for all three masses and two example mixing values.

Table 4.2: Three dimensional binning used in the analysis. All variables are from the FLERCNN reconstruction explained in Section ??.

| Variable | N_{bins} | Edges | Step |
|----------------|-------------------|--------------------------|-------------|
| P_ν | 3 | [0.00, 0.25, 0.55, 1.00] | linear |
| E | 12 | [5.00, 100.00] | logarithmic |
| $\cos(\theta)$ | 8 | [-1.00, 0.04] | linear |

4.1.2 Analysis Binning

[26]: Yu et al. (2023), “Recent neutrino oscillation result with the IceCube experiment”

add 3D expectation and/or S/sqrt(B) plots

The identical binning to the analysis performed in [26] is used. It was chosen such that the track-like bin has the largest ν_μ -CC fraction. Extend the binning towards lower energies or increasing the number of bins did not improve the HNL sensitivities significantly. It also has to be considered that sufficient data events need to end up in the individual bins to result in a good fit, which was already investigated in the previous analysis. To mitigate the low data statistics, a few bins were not taken into account in the analysis. There are three bins in PID (cascade-like, mixed and track-like), 12 bins in reconstructed energy, and 8 bins in cosine of the reconstructed zenith angle as specified in Table 4.2. Originally, there were two more bins in $\cos(\theta)$, which were removed to reduce muons coming from the horizon and some low energy bins in the cascade-like bin are removed due to the low event expectation.

4.2 Statistical Analysis

4.2.1 Test Statistic

The measurements are performed by comparing the weighted MC to the data. Through variation of the nuisance and physics parameters that govern the weights, the best matching set of parameters can be found. The comparison is done using a modified χ^2 defined as

$$\chi^2_{\text{mod}} = \sum_{i \in \text{bins}} \frac{(N_i^\nu + N_i^\mu + N_i^{\text{HNL}} - N_i^{\text{obs}})^2}{N_i^\nu + N_i^\mu + N_i^{\text{HNL}} + (\sigma_i^\nu)^2 + (\sigma_i^\mu)^2 + (\sigma_i^{\text{HNL}})^2} + \sum_{j \in \text{syst}} \frac{(s_j - \hat{s}_j)^2}{\sigma_{s_j}^2}, \quad (4.1)$$

as the test statistic (TS), where N_i^ν , N_i^μ , and N_i^{HNL} are the expected number of events in bin i from neutrinos, atmospheric muons, and HNL, while N_i^{obs} is the observed number of events in bin i . The expected number of events from each particle type is calculated by summing the weights of all events in the bin $N_i^{\text{type}} = \sum_i^{\text{type}} \omega_i$, with the statistical uncertainty being $(\sigma_i^{\text{type}})^2 = \sum_i^{\text{type}} \omega_i^2$. The expected Poisson error is calculated using the combined expectation of neutrinos, atmospheric muons, and HNL events. The additional term in Equation 4.1 is included to apply a penalty term for prior knowledge of the systematic uncertainties of the parameters where they are known. s_j are the systematic parameters that are varied in the fit, while \hat{s}_j are their nominal values and σ_{s_j} are the known uncertainties.

Do I want/need to include the description of the KDE muon estimation?

Add table with all systematic uncertainties used in this analysis (in the analysis chapter).

add final level effects of varying the axial mass parameters (or example of one)

add final level effects of varying the DIS parameter (or example of one)

4.2.2 Systematic Uncertainties

4.3 Analysis Checks

Fitting to data will be performed in a *blind* manner, where the analyzer does not immediately see the fitted physics and nuisance parameter values, but first checks that a set of pre-defined *goodness of fit* (*GOF*) criteria are fulfilled. If those criteria are met to satisfaction the fit results are unblinded and the full result can be revealed. Before these blind fits to data are run, the robustness of the analysis method is tested using pseudo-data that is generated using the MC sets.

4.3.1 Minimization Robustness

To find the set of parameters that describes the data best, a staged minimization routine is used. In the first stage, a fit with coarse minimizer settings is performed to find a rough estimate of the *best fit point* (*BFP*). In the second stage, the fit is performed again in both octants¹ of θ_{23} , starting from the BFP of the coarse fit. For each individual fit the *MIGRAD* routine of *IMINUIT* [27] is used to minimize the χ^2 TS defined in Equation 4.1. *Iminuit* is a fast, python compatible minimizer based on the *Minuit2* C++ library [28]. The individual minimizer settings are shown in Table 4.3.

To test the minimization routine and to make sure it consistently recovers any injected physics parameters, pseudo-data sets are produced from the MC by choosing the nominal nuisance parameters and specific physics parameters, without adding any statistical or systematic fluctuations to it. These so-called *Asimov*² data sets are then fit back with the full analysis chain. This type of test is called *Asimov inject/recover test*. A set of mixing values between 10^{-3} and 10^0 is injected and fit back. Even though this range is well within the excluded regions by other experiments, discussed in Section 1.4.4, this covers the current sensitive region of the analysis in IceCube DeepCore. Without fluctuations the fit is expected to always recover the injected parameters (both physics and nuisance parameters). The fitted mixing values from the Asimov inject/recover tests are compared to the true injected values in Figure 4.1 for the 0.6 GeV set. As expected, the fit is always able to recover the injected physcis parameter and the nuisance paramters. Additional plots for the other mass sets can be found in Section ??.

4.3.2 Ensemble Tests

To estimate the goodness of fit, pseudo-data is generated from the MC by injecting the BFP parameters as true parameters and then fluctuating the expected bin counts using Poisson fluctuation. The resulting pseudo-data sets are then fit back with the analysis chain. By comparing the distribution of TS values from this *ensemble* of pseudo-data trials to the TS of the fit to real data, a p-value can be calculated. The p-value is the probability of finding a TS value at least as large as the one from the data fit. Figure 4.2 shows the TS distribution from the ensemble tests for the 0.6 GeV mass set and the observed TS value from the fit, resulting in a p-value of 1.23 %³. Plots for the addition two mass sets are shown in Section ??.

1: There is a degeneracy between the lower octant ($\theta_{23} < 45^\circ$) and the upper octant ($\theta_{23} > 45^\circ$), which can lead to TS minima (local and global) at two positions that are mirrored around 45° in θ_{23} .

[27]: Dembinski et al. (2022), *scikit-hep/iminuit*: v2.17.0

[28]: James et al. (1975), “Minuit: A System for Function Minimization and Analysis of the Parameter Errors and Correlations”

| Fit | Err. | Prec. | Tol. |
|--------|------|-------|------|
| Coarse | 1e-1 | 1e-8 | 1e-1 |
| Fine | 1e-5 | 1e-14 | 1e-5 |

Table 4.3: Migrad settings for the two stages in the minimization routine. *Err.* are the step size for the numerical gradient estimation, *Prec.* is the precision with which the LLH is calculated, and *Tol.* is the tolerance for the minimization.

2: A pseudo-data set without statistical fluctuations is called Asimov data set.

Do I want additional plots for this (fit diff, LLH distr, minim. stats, param. fits)?

Add bin-wise TS distribution? Add 3D TS maps?

3: The p-values for the 0.3 GeV and 1.0 GeV are 1.23 % and 1.23 %, respectively

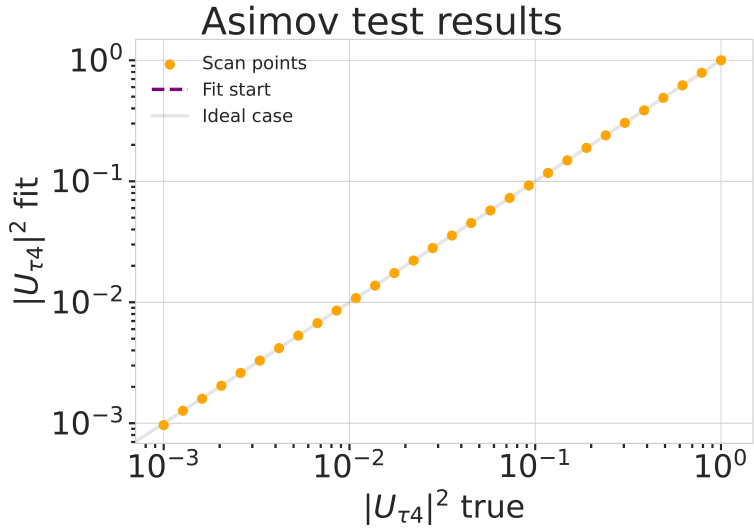


Figure 4.1: Asimov inject/recover test for the 0.6 GeV mass set. Mixing values between 10^{-3} and 10^0 are injected and fit back with the full analysis chain. The injected parameter is always recovered within the statistical uncertainty.

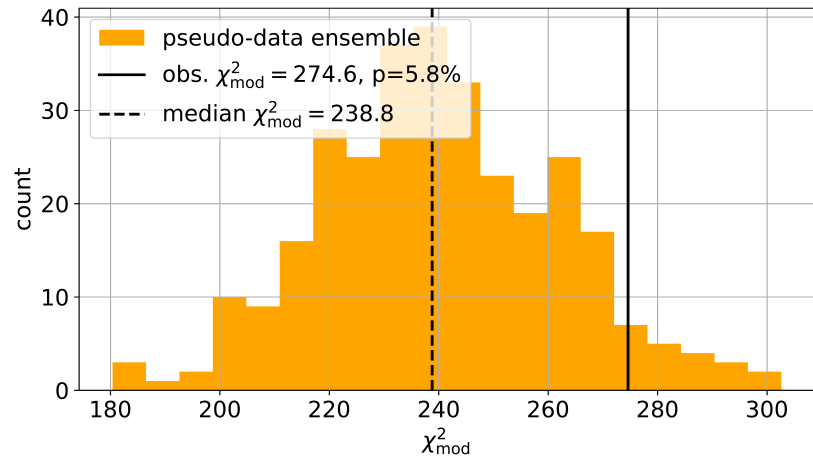


Figure 4.2: Observed fit TS and TS distribution from pseudo-data trials for the 0.6 GeV mass set.

4.4 Results

4.4.1 Best Fit Parameters

4.4.2 Upper Limits

4.4.3 Post-Fit Data/MC Agreement

4.4.4 Likelihood Coverage

Bibliography

Here are the references in citation order.

- [1] M. Thomson. *Modern particle physics*. Cambridge [u.a.]: Cambridge University Press, 2013, XVI, 554 S. (Cited on pages 1, 2).
- [2] S. L. Glashow. "Partial-symmetries of weak interactions". In: *Nuclear Physics* 22.4 (1961), pp. 579–588. doi: [https://doi.org/10.1016/0029-5582\(61\)90469-2](https://doi.org/10.1016/0029-5582(61)90469-2) (cited on page 1).
- [3] M. Tanabashi et al. "Review of Particle Physics". In: *Phys. Rev. D* 98 (3 Aug. 2018), p. 030001. doi: [10.1103/PhysRevD.98.030001](https://doi.org/10.1103/PhysRevD.98.030001) (cited on pages 2, 8, 9).
- [4] A. Terliuk. "Measurement of atmospheric neutrino oscillations and search for sterile neutrino mixing with IceCube DeepCore". PhD thesis. Berlin, Germany: Humboldt-Universität zu Berlin, Mathematisch-Naturwissenschaftliche Fakultät, 2018. doi: [10.18452/19304](https://doi.org/10.18452/19304) (cited on pages 2, 4).
- [5] J. A. Formaggio and G. P. Zeller. "From eV to EeV: Neutrino cross sections across energy scales". In: *Rev. Mod. Phys.* 84 (3 Sept. 2012), pp. 1307–1341. doi: [10.1103/RevModPhys.84.1307](https://doi.org/10.1103/RevModPhys.84.1307) (cited on page 3).
- [6] T. Yanagida. "Horizontal Symmetry and Masses of Neutrinos". In: *Progress of Theoretical Physics* 64.3 (Sept. 1980), pp. 1103–1105. doi: [PTP.64.1103](https://doi.org/10.1103/PTP.64.1103) (cited on page 4).
- [7] P. Astier et al. "Search for heavy neutrinos mixing with tau neutrinos". In: *Phys. Lett. B* 506 (2001), pp. 27–38. doi: [10.1016/S0370-2693\(01\)00362-8](https://doi.org/10.1016/S0370-2693(01)00362-8) (cited on page 5).
- [8] R. Acciari et al. "New Constraints on Tau-Coupled Heavy Neutral Leptons with Masses mN=280–970 MeV". In: *Phys. Rev. Lett.* 127.12 (2021), p. 121801. doi: [10.1103/PhysRevLett.127.121801](https://doi.org/10.1103/PhysRevLett.127.121801) (cited on page 5).
- [9] J. Orloff, A. N. Rozanov, and C. Santoni. "Limits on the mixing of tau neutrino to heavy neutrinos". In: *Phys. Lett. B* 550 (2002), pp. 8–15. doi: [10.1016/S0370-2693\(02\)02769-7](https://doi.org/10.1016/S0370-2693(02)02769-7) (cited on page 5).
- [10] I. Boiarska et al. "Blast from the past: constraints from the CHARM experiment on Heavy Neutral Leptons with tau mixing". In: (July 2021) (cited on page 5).
- [11] P. Abreu et al. "Search for neutral heavy leptons produced in Z decays". In: *Z. Phys. C* 74 (1997). [Erratum: *Z.Phys.C* 75, 580 (1997)], pp. 57–71. doi: [10.1007/s002880050370](https://doi.org/10.1007/s002880050370) (cited on page 5).
- [12] P. Coloma et al. "Double-Cascade Events from New Physics in Icecube". In: *Phys. Rev. Lett.* 119.20 (2017), p. 201804. doi: [10.1103/PhysRevLett.119.201804](https://doi.org/10.1103/PhysRevLett.119.201804) (cited on page 4).
- [13] P. Coloma. "Icecube/DeepCore tests for novel explanations of the MiniBooNE anomaly". In: *Eur. Phys. J. C* 79.9 (2019), p. 748. doi: [10.1140/epjc/s10052-019-7256-8](https://doi.org/10.1140/epjc/s10052-019-7256-8) (cited on page 4).
- [14] P. Coloma et al. "GeV-scale neutrinos: interactions with mesons and DUNE sensitivity". In: *Eur. Phys. J. C* 81.1 (2021), p. 78. doi: [10.1140/epjc/s10052-021-08861-y](https://doi.org/10.1140/epjc/s10052-021-08861-y) (cited on pages 5, 7, 15, 17, 18).
- [15] M. Honda et al. "Atmospheric neutrino flux calculation using the NRLMSISE-00 atmospheric model". In: *Phys. Rev. D* 92 (2 July 2015), p. 023004. doi: [10.1103/PhysRevD.92.023004](https://doi.org/10.1103/PhysRevD.92.023004) (cited on page 8).
- [16] A. Fedynitch et al. "Calculation of conventional and prompt lepton fluxes at very high energy". In: *European Physical Journal Web of Conferences*. Vol. 99. European Physical Journal Web of Conferences. Aug. 2015, p. 08001. doi: [10.1051/epjconf/20159908001](https://doi.org/10.1051/epjconf/20159908001) (cited on page 8).
- [17] M. Honda et al. "Calculation of atmospheric neutrino flux using the interaction model calibrated with atmospheric muon data". In: *Phys. Rev. D* 75 (4 Feb. 2007), p. 043006. doi: [10.1103/PhysRevD.75.043006](https://doi.org/10.1103/PhysRevD.75.043006) (cited on page 8).
- [18] S. Bilenky and B. Pontecorvo. "Lepton mixing and neutrino oscillations". In: *Physics Reports* 41.4 (1978), pp. 225–261. doi: [10.1016/0370-1573\(78\)90095-9](https://doi.org/10.1016/0370-1573(78)90095-9) (cited on page 9).

- [19] P. A. M. Dirac. "The Quantum Theory of the Emission and Absorption of Radiation". In: *Proceedings of the Royal Society of London Series A* 114.767 (Mar. 1927), pp. 243–265. doi: [10.1098/rspa.1927.0039](https://doi.org/10.1098/rspa.1927.0039) (cited on page 9).
- [20] G. Van Rossum and F. L. Drake. *Python 3 Reference Manual*. Scotts Valley, CA: CreateSpace, 2009 (cited on page 11).
- [21] R. Abbasi et al. "LeptonInjector and LeptonWeighter: A neutrino event generator and weighter for neutrino observatories". In: *Comput. Phys. Commun.* 266 (2021), p. 108018. doi: [10.1016/j.cpc.2021.108018](https://doi.org/10.1016/j.cpc.2021.108018) (cited on page 15).
- [22] J. Alwall et al. "The automated computation of tree-level and next-to-leading order differential cross sections, and their matching to parton shower simulations". In: *JHEP* 07 (2014), p. 079. doi: [10.1007/JHEP07\(2014\)079](https://doi.org/10.1007/JHEP07(2014)079) (cited on page 16).
- [23] C. Argüelles. <https://github.com/arguelles/NuXSSplMkr> (cited on page 16).
- [24] J.-M. Levy. "Cross-section and polarization of neutrino-produced tau's made simple". In: *J. Phys. G* 36 (2009), p. 055002. doi: [10.1088/0954-3899/36/5/055002](https://doi.org/10.1088/0954-3899/36/5/055002) (cited on page 16).
- [25] E. Tiesinga et al. "CODATA recommended values of the fundamental physical constants: 2018". In: *Rev. Mod. Phys.* 93 (2 July 2021), p. 025010. doi: [10.1103/RevModPhys.93.025010](https://doi.org/10.1103/RevModPhys.93.025010) (cited on page 17).
- [26] S. Yu and J. Micallef. "Recent neutrino oscillation result with the IceCube experiment". In: *38th International Cosmic Ray Conference*. July 2023 (cited on page 24).
- [27] H. Dembinski et al. *scikit-hep/iminuit: v2.17.0*. Version v2.17.0. Sept. 2022. doi: [10.5281/zenodo.7115916](https://doi.org/10.5281/zenodo.7115916) (cited on page 25).
- [28] F. James and M. Roos. "Minuit: A System for Function Minimization and Analysis of the Parameter Errors and Correlations". In: *Comput. Phys. Commun.* 10 (1975), pp. 343–367. doi: [10.1016/0010-4655\(75\)90039-9](https://doi.org/10.1016/0010-4655(75)90039-9) (cited on page 25).